npj | Materials Degradation

www.nature.com/npjmatdeg

ARTICLE OPEN

Check for updates

Influence of TiO_2 pigment particles on chromate ion transport in epoxy films

Małgorzata Kopeć[1]✉, Brenda D. Rossenaar[1], Kees van Leerdam[1], Arne Janssen[1], Antony N. Davies[1,2], Stuart B. Lyon[3], Peter Visser[4] and Simon R. Gibbon[5]

Transport of active species (i.e., ions) leaching from pigment particles incorporated in a polymer matrix is the main mechanism behind the anticorrosive performance of protective coatings. Understanding this mechanism is necessary for the effective design of the systems utilizing pigments less toxic than the most efficient chromate salts. It was demonstrated that anticorrosive pigment particles can themselves facilitate the transport of active species via the pathways formed after pigment leaching from a coating. It was also suggested that other paint components, e.g., certain additives, pigments, and fillers can be involved in the formation of transport pathways. Investigation of the possible influence of inert pigment (TiO_2) on creating the pathways for chromate ion transport in polymer coatings was the primary objective of this work. In an experiment mimicking the transport of pigment species (i.e., chromate ions), a model epoxy coating containing particles of a single pigment (TiO_2) was exposed to a chromate solution (aqueous, or with the addition of acetone as a polymer swelling agent). It was shown that the chromate ions can be transported in the epoxy film preferentially via the TiO_2 particles/polymer matrix interface.

npj Materials Degradation (2021)5:9 ; https://doi.org/10.1038/s41529-021-00156-7

INTRODUCTION

Despite decades of research, there is still some doubt about how corrosion-protective organic coatings work[1]. Two commonly accepted mechanisms state that corrosion protection occurs either by the formation of a barrier to external corrosive species or by the blocking of charge transfer between anode and cathode areas on a metal surface due to the high volumetric resistivity of the polymer binder (or by a combination of these mechanisms)[2]. Polymer coatings are generally formulated to contain functional pigments (including anticorrosive agents such as corrosion inhibitors), additives, and nonfunctional fillers, dispersed in the coating volume[3]. Active corrosion protection is a key benefit of such systems that allow mitigation of the substrate corrosion that can occur during the service lifetime upon, e.g., coating damage or aging. Generally, anticorrosive pigments are incorporated into coatings, where active species (i.e., ions) leach in presence of water and migrate to the metallic substrate resulting in inhibition of the corrosion process[4]. Effective pigments have limited solubility in water to prevent excessive leaching and provide long-term release over the entire service time. Leachable chromate pigments are commonly included in the best-performing anticorrosive coatings[5,6]. However, other solutions are being searched for due to the highly toxic properties of chromates[7–9], but one of the key obstacles for the effective design of chromate-free anticorrosive coatings is that most alternatives are just not as effective. Although the diffusion of water within polymer membranes is well-studied[10,11], the migration of ions within polymers and the localization of water and ions at polymer interfaces with solid second phases, such as pigments, additives, and substrates, is not well-understood. It is commonly assumed that water diffuses into polymers via its free volume; however, ionic transport is less understood as this must occur via a solvation mechanism. It has been proposed that ions migrate via interconnected pathways the formation of which is not fully understood[12–15]. Of course, how ionic inhibitive species leach from pigments and migrate to corroding surfaces is fundamental to how active corrosion protection works[1].

The rate of migration of the pigment species from coatings can be measured indirectly, i.e., by leaching experiments, where the pigmented samples are exposed to deionized water or an electrolyte solution containing, for example, NaCl. However, where pigments are known to act via ion exchange, the use of deionized water will prevent the release of active species. The concentration of leached inhibitor into the solution after exposure can be measured using techniques, such as ion chromatography or inductively coupled plasma mass spectrometry (ICP-MS)[16,17]. The distribution of pigments in a coating matrix and depletion depth as a result of inhibitor leaching may also be characterized by methods like Raman spectroscopy or scanning electron microscopy/energy-dispersive X-ray spectroscopy (SEM/EDS), as well as 3D imaging methods, such as X-ray computational tomography (XCT) or SEM-based 3D-sectioning techniques[15,18].

Recently, leaching of anticorrosive pigment particles ($SrCrO_4$) has been studied from a model epoxy coating upon exposure to a NaCl solution using tomography techniques. The uneven depletion depth of particles leached out during exposure, and the low level of chromate within the polymer matrix suggested that pigment species did not diffuse significantly into the epoxy[19,20]. It is commonly assumed that the size of a chromate ion, which is of the same order as the free volume in the polymer, prevents transport through the coating matrix[21]. A proposed mechanism of pigment leaching assumed that the particles exposed to the environment via the coating surface leached first. Leaching of the other particles from the coating was via transport through a network of connected voids formed after dissolution of $SrCrO_4$ clusters. This was demonstrated by a 3D distribution study of

[1]Nouryon, Deventer, The Netherlands. [2]Sustainable Environment Research Centre, Faculty of Computing, Engineering and Science, University of South Wales, Pontypridd, UK. [3]Corrosion and Protection Centre, School of Materials, the University of Manchester, Manchester, UK. [4]AkzoNobel, Research & Development, Sassenheim, The Netherlands. [5]AkzoNobel, Research & Development, Stoneygate Lane, Felling, Gateshead, Tyne & Wear, UK. ✉email: malgorzata.kopec@airbus.com

Published in partnership with CSCP and USTB

npj nature partner journals

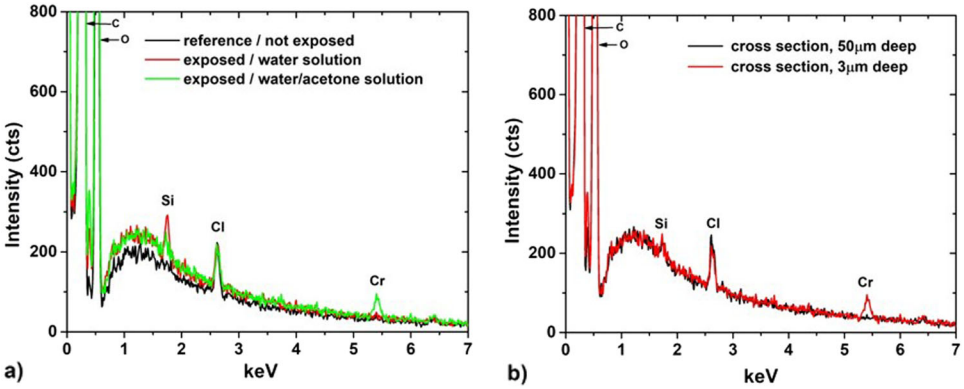

Fig. 1 EDS spectra of unpigmented epoxy films. a Comparison of EDS spectra for the reference (unexposed) film and for films after exposure to Na_2CrO_4 solution in water and water/acetone for 24 h at 60 °C (measured in the top region of the films close to the surface). **b** Comparison of EDS spectra measured in the top and the middle region of a cross section of an unpigmented epoxy film after exposure to Na_2CrO_4 solution in water/acetone for 24 h at 60 °C.

inhibitor particles with XCT and serial block-face SEM showing that the pigment particles formed connected structures in the polymer matrix[22].

However, evidence for leaching of unconnected pigment particles has also been observed, suggesting migration through other pathways. Connected clusters of other particles included in the coating, such as TiO_2, which themselves remain inert to dissolution, were considered; however, no evidence was found for such mechanism[23].

Current analytical methods do not allow direct, real-time observation of the movement of ions in polymer films[24]. In addition, analysis of data obtained non-directly from the leaching experiments is challenging for complex fully formulated systems with many additives which role in the transport is not understood.

Recently, we proposed an experimental approach that allowed focusing on one type of additive used in the formulation of coatings and studying its potential role in the transport of chromate ions[25]. Simplified model epoxy films with the addition of one type of particle ($BaSO_4$) were used to study the transport of chromate ions into the coating from an external solution. $BaSO_4$ particles were shown to actively contribute to the chromate ion migration via an ion-exchange mechanism while slowly leaching from the film. A similar methodology was applied in this paper to study the influence of inert pigment particles (TiO_2) on chromate ion transport in epoxy films immersed in chromate solutions at different conditions.

Unpigmented and TiO_2-containing films at pigment volume concentration (PVC) of 30 and 50% ($30TiO_2$ and $50TiO_2$, respectively) were exposed at temperatures below and above the T_g of the polymer and with the addition of acetone to act as a swelling agent. Both PVCs were above the theoretical percolation threshold, which is 15.7% for randomly distributed spheres[26]. $30TiO_2$ film was expected to be internally connected via the polymer, while $50TiO_2$ film was in the range of the critical volume concentration for TiO_2 pigment where particles not fully covered by the resin are likely to be present in the film[27,28]. SEM/EDS and scanning transmission electron microscopy/EDS (STEM/EDS) were used for examination of the morphology and elemental analysis of the films after exposure.

RESULTS AND DISCUSSION

Unpigmented films exposed to Na_2CrO_4 solutions

Unpigmented epoxy films were tested as a reference for further experiments with TiO_2-filled films. After exposure, the films were visually inspected to record any changes. The film exposed to the aqueous solution of Na_2CrO_4 for 24 h at 60 °C remained transparent while the film exposed to the chromate solution in the water/acetone mixture took up the yellow hue of the chromate solution (see Supplementary Fig. 1). This suggested a higher uptake of chromate into the film where acetone was present in the external environment as a film plasticizer.

For further analysis using SEM/EDS, the films were cut using an ultramicrotome to obtain uniform smooth cross sections. The comparison of EDS spectra of the film after exposure to Na_2CrO_4 solution in water and water/acetone for 24 h at 60 °C and an unexposed reference film is presented in Fig. 1a. The characteristic Cr peak (Kα 5.4 keV) is apparent only in the spectra of the film exposed to the chromate solution in water/acetone. Silicon peak (Kα 1.7 keV) arising from adventitious contamination, was also evident at the limit of detection.

The chemical composition of an unexposed film was measured at the cross section at 1/2 of the film thickness by SEM/EDS. The elements identified in the film were C, O, and Cl at average concentrations of 83.0, 16.6, and 0.3 wt. %, respectively (Supplementary Table 1).

In the case of films exposed to chromate solutions, EDS spectra were acquired at different film depths (see Supplementary Fig. 2). Based on the EDS spectra, the average concentration of elements was calculated for three different points at the same depth. In the case of the film exposed to aqueous chromate solution, the concentrations of C, O, and Cl were similar to the composition of an unexposed sample, independent of the depth (Supplementary Table 2). No Cr was detected in the sample, indicating either that the migration of chromate into the film did not occur or that the Cr concentration was below the detection limit of EDS. The same was concluded for the unpigmented films exposed to an aqueous Na_2CrO_4 solution in different conditions (14 days at 60 °C and 6 weeks at RT) and these samples are not further considered in this paper.

Figure 1b presents the comparison of the spectra measured at distances of 3 and 50 μm from the surface of the film exposed to Na_2CrO_4 solution in water/acetone mixture for 24 h at 60 °C. The characteristic Cr peak is clearly seen in the spectrum at the depth of 3 μm but is not visible at 50 μm. EDS data showed that the concentrations of C, O, Cl, and Si were similar as in the unexposed film. In addition, Cr was clearly detected with its level depending on the distance from the surface (Supplementary Table 3). Quantification of the EDS data indicates that close to the surface the Cr level was highest (~0.6 wt. % Cr at 3 μm depth), which gradually decreased down to 0.1 wt. % at 25 μm depth (Table 1); deeper into the film (50 μm) no Cr was found.

Cr was detected in the unpigmented film exposed to the chromate solution containing acetone at the temperature above T_g but not in the film exposed to the fully aqueous solution. In the temperature above T_g, the addition of acetone promotes polymer

swelling hence aiding the ingress of chromate into the film[29]. On the other hand, Cr was below the detection limit in the films exposed to aqueous solutions even when immersion was extended to 6 weeks at RT and up to 14 days at 60 °C. It is commonly assumed that chromate ions cannot penetrate an epoxy matrix due to size exclusion. For an epoxy system similar to the one used in this investigation, the free volume pore radius is reported to be 0.29 nm[17,18], the radius of the anhydrous CrO_4^{2-} anion is 0.229 nm[30], and the radius of the hydrated anion is calculated as 0.525 nm[31]. Based solely on size, penetration of hydrated chromate via polymer-free volume indeed does not seem possible, however, the migration of ions in polymers depends on the ionic interaction and is not fully understood[32].

TiO_2-filled films exposed to Na_2CrO_4 solution with acetone

As for the unpigmented film, the pigmented $30TiO_2$ sample changed color after exposure to Na_2CrO_4 solution with acetone addition for 24 h at 60 °C (see Supplementary Fig. 3). SEM analysis of the surface and cross sections of the films before and after exposure was performed. Most of the TiO_2 particles appeared fully coated with the polymer (Fig. 2a, b). The cross-sectional analysis showed a uniform distribution of the particles in the films (Fig. 2c, d). After exposure, the particle size ($d = 100–200$ nm) and shape remained the same as in the unexposed film.

Figure 2e compares the SEM/EDS spectra of $30TiO_2$ film: the unexposed and after exposure to Na_2CrO_4 solution in the water/acetone mixture where chromium was additionally detected in the film. C, O, Ti, and Al were detected in the unexposed film (Supplementary Table 4). Where present, Al originated from the surface additives were used to modify TiO_2[26,33].

The spectra were acquired at three different points at the same depths as for the unpigmented film and Cr was detected when exposed to the acetone-containing solution for 24 h of at 60 °C (Supplementary Table 5). Cr was detected up to 50 µm of the film depth showing chromate had penetrated considerably deeper than in the unpigmented film (Table 2). The concentration of Cr

Table 1. Concentration of Cr at different sample depths for epoxy film exposed to Na_2CrO_4 solution in water/acetone for 24 h at 60 °C.

Sample depth (µm)[a]	Cr (wt. %) point 1	Cr (wt. %) point 2	Cr (wt. %) point 3	Cr (wt. %) average	s (±)
3	0.6	0.7	0.6	0.6	0.06
5	0.5	0.5	0.5	0.5	0
15	0.2	0.2	0.2	0.2	0
25	0.1	0.1	0.1	0.1	0
50	–	–	–	–	–

[a]Composition of the sample at different depths is reported up to half of its thickness (50 µm); the film was exposed from both sides, hence the maximum migration distance equals to 1/2 of the sample thickness. The thickness of the film was 100 µm.

Table 2. Concentration of Cr at different depths of $30TiO_2$ film after exposure to Na_2CrO_4 solution in water/acetone for 24 h at 60 °C.

Sample depth (µm)[a]	Cr (wt. %) point 1	Cr (wt. %) point 2	Cr (wt. %) point 3	Cr (wt. %) average	s (±)
3	0.2	0.3	0.3	0.3	0.08
6	0.4	0.2	0.4	0.3	0.12
12	0.5	0.4	0.4	0.4	0.06
25	0.2	0.3	0.5	0.3	0.15
50	0.2	0.3	0.2	0.2	0.06

[a]Composition of the film at different depths is reported up to half of its thickness (50 µm); the film was exposed from both sides, hence the maximum migration distance equals to 1/2 of the film thickness. The thickness of the film was 100 µm.

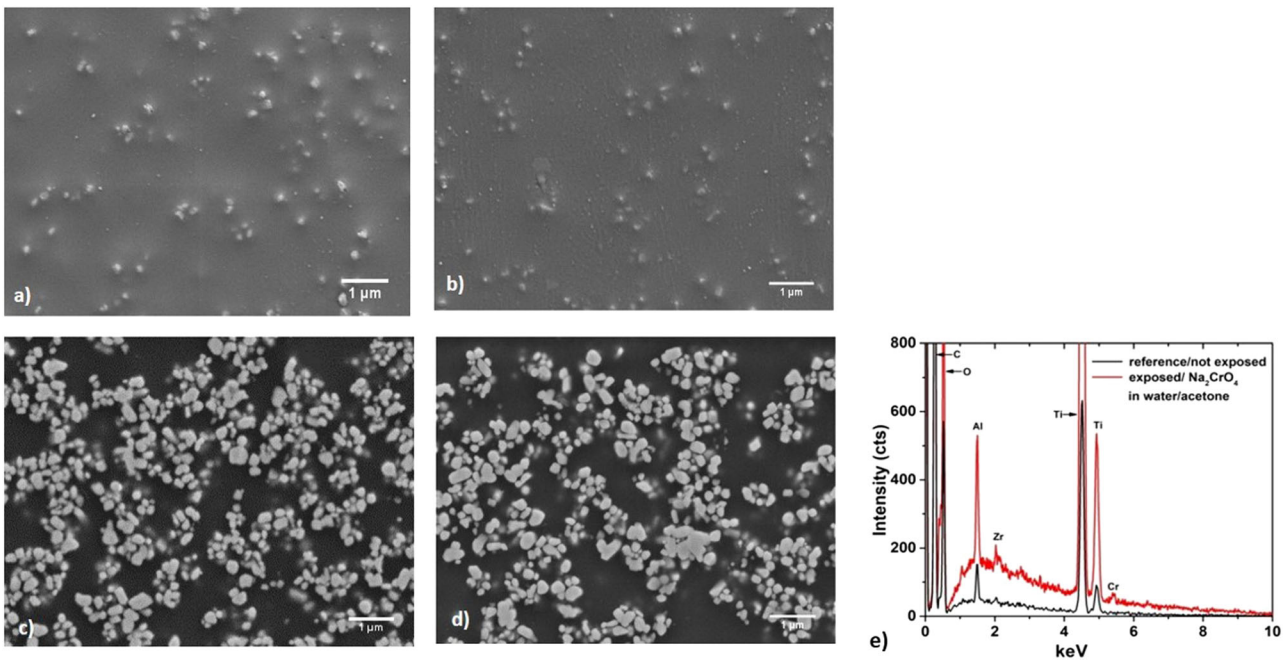

Fig. 2 SEM/EDS analysis of $30TiO_2$ films. a SEM image of $30TiO_2$ surface before exposure. **b** SEM image of $30TiO_2$ surface after 24 h exposure to Na_2CrO_4 solution in water/acetone at 60 °C. **c** SEM image of $30TiO_2$ cross section before exposure. **d** SEM image of $30TiO_2$ cross section after 24 h exposure to Na_2CrO_4 solution in water/acetone at 60 °C. **e** Comparison of EDS spectra measured at the cross section at 1/2 of the $30TiO_2$ film thickness before and after exposure to the Na_2CrO_4 solution in water/acetone mixture for 24 h at 60 °C. The thickness of the film is 100 µm.

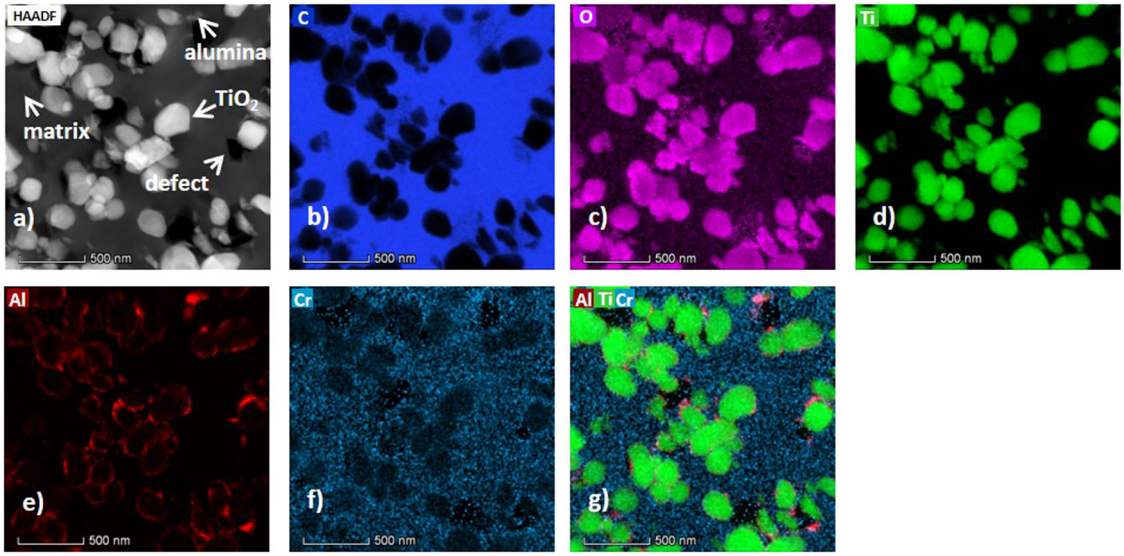

Fig. 3 STEM/EDS analysis of $30TiO_2$ film after exposure to Na_2CrO_4 solution in water/acetone for 24 h at 60 °C. a STEM lamella of $30TiO_2$ film after exposure to Na_2CrO_4 solution in water/acetone for 24 h at 60 °C. **b–f** Distribution of C, O, Ti, Al, and Cr, respectively. **g** Overlay of the distribution of Al, Ti, and Cr.

within the film was uniform indicating saturation of the film with the solution.

For polymer materials such as investigated films, the sampling volume in SEM/EDS analysis at typically used voltage can reach 2 µm[34]. As this is significantly larger than the TiO_2 particle size (100–200 nm of diameter), it is not possible to separate TiO_2 and polymer matrix signals using SEM/EDS. Every measurement point, therefore, consists of a combination of signals from both phases, the ratio of which may vary (see Supplementary Discussion for more details). Due to the sampling volume of the electron beam interacting with the polymer material, it is also difficult to determine if Cr is located within the matrix or on the TiO_2 particles. Analytical resolution can be improved using STEM/EDS where the thin sample limits the spread of the incident electron beam. Sections, of thickness ~70 nm, were thus imaged at the center of the film depth (Fig. 3a). The TiO_2 particles are clearly visible in the polymer matrix as well as other features (smaller with lower contrast) that were identified as alumina. Such material is associated with the TiO_2 pigment as it is used for modification of the particle's surface[33]. The spectral images show the distribution of C, O, Ti, Al, and Cr in the investigated area (Fig. 3b–f), where C represents the polymer matrix, Ti and O correspond to TiO_2 particles, while Al is concentrated mostly at the surface of the pigment particles. Significantly, Cr appears to be evenly distributed in the polymer matrix. An overlay of the Ti, Al, and Cr distribution shows alumina (red) located on the surface of TiO_2 (green) or in the matrix (detached from the particle surface) and Cr (blue) uniformly distributed in the matrix (Fig. 3g). The quantitative chemical composition of the analyzed area was in good agreement with SEM/EDS results (Supplementary Tables 5 and 6).

A STEM/EDS analysis with higher magnification was performed to evaluate the exact location of the elements. As seen in Fig. 4, Al is concentrated at the TiO_2 particle surface while Cr is uniformly distributed in the polymer matrix.

The results suggest that, in the water–acetone environment at a temperature above T_g, the film was penetrated with the chromate by ion transport mainly via the polymer matrix. The Cr penetration depth was twice as high as in the unpigmented film after the same length of exposure. This indicated that Cr was transported further (more rapidly) into the pigmented film than in the pure polymer. The morphology and chemical composition of the TiO_2 particles did not change after exposure, indicating that the presence of the particles in the film accelerated the chromate transport without significant interaction with the solution. A key factor allowing chromate transport within the film was the increased swelling of the polymer matrix with acetone; however, the pigmented film reached an equilibrium with the chromate solution faster than the unpigmented film. After 24 h of exposure, the film was in equilibrium with the solution and the concentration of Cr was uniform in the entire polymer film. The fact that chromate penetrated pigmented film twice faster than pure polymer film allows concluding that in the pigmented film must be short-circuit pathways for chromate migration. These pathways are postulated to be located at the interface of the interconnected particles (at the volume above theoretical percolation threshold) and polymer matrix as suggested for water transport in a model composite system[35]. However, the pathways could not be observed since the tested films reached equilibrium with chromate solution and Cr was uniformly distributed.

In summary, Cr was detected within the unpigmented film (i.e., within the polymer) after exposure for 24 h at 60 °C to Na_2CrO_4 solution when acetone was added. This suggested the transport of chromate in the film was facilitated by the interaction of acetone with the polymer matrix presumably due to film swelling. Similarly, Cr was detected in $30TiO_2$ film; however, the Cr had penetrated twice as deep into the pigmented film compared to the unpigmented film. Under these conditions, Cr was present predominantly within the polymer matrix and not segregated to the pigment/matrix interface. Thus, in the presence of pigment, chromate penetration into the film was accelerated however the mechanism of transport in comparison to transport via a pure polymer was not changed.

TiO_2-filled films exposed to aqueous Na_2CrO_4 solution

Cr was not detected in the unpigmented films exposed to aqueous Na_2CrO_4 solution independently of the time and temperature of exposure (1–14 days at 60 °C and up to 6 weeks at RT). Films pigmented with TiO_2 at PVC of 30 and 50% (i.e., respectively, below and in the range of critical PVC) were exposed in the same conditions as unpigmented films. SEM/EDS analysis was performed at the cross sections of the films after exposure. Cr was detected only in $50TiO_2$ film after 14 days exposure at 60 °C but not in any other tested film (Fig. 5e). Analysis of the surface and cross sections of $50TiO_2$ film before and after exposure was

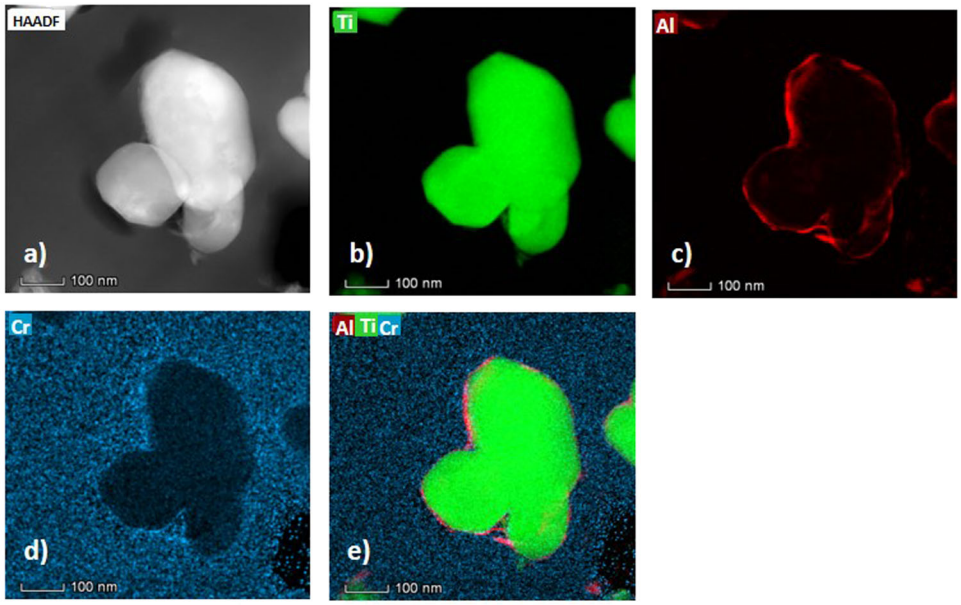

Fig. 4 High-magnification STEM/EDS analysis of $30TiO_2$ film after exposure to Na_2CrO_4 solution in water/acetone for 24 h at 60 °C. a STEM lamella of $30TiO_2$ film after exposure to Na_2CrO_4 solution in water/acetone for 24 h at 60 °C. **b**–**d** Distribution of Ti, Al, and Cr, respectively. **e** Overlay of the distribution of Al, Ti, and Cr.

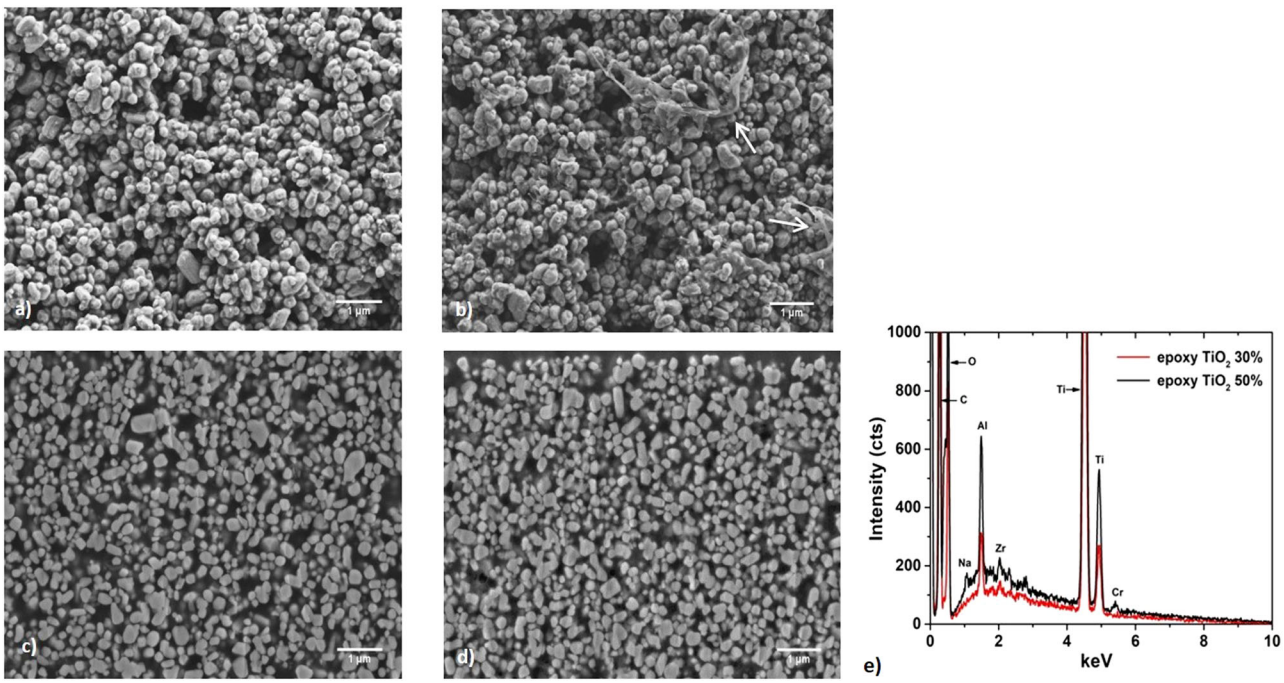

Fig. 5 SEM/EDS analysis of $50TiO_2$ film after 14 days of exposure to aqueous Na_2CrO_4 solution at 60 °C. a SEM image of $50TiO_2$ surface before exposure. **b** SEM image of $50TiO_2$ surface after 14 days of exposure to aqueous Na_2CrO_4 solution at 60 °C. **c** SEM image of $50TiO_2$ cross section before exposure. **d** SEM image of $50TiO_2$ cross section after 14 days of exposure to aqueous Na_2CrO_4 solution at 60 °C. **e** EDS spectra from the middle part of the cross sections of $50TiO_2$ and $30TiO_2$ films after exposure to the aqueous solution of Na_2CrO_4 for 14 days at 60 °C.

performed. As expected for a film containing pigment in the range of the critical PVC, the surface of the film was rough, showing TiO_2 particles stacking upon each other, only covered with a thin layer of polymer (Fig. 5a). The morphology after exposure was similar to that prior to exposure; however, some thin fragments of polymer peeled off from the surface were identified (Fig. 5b). Analysis of the cross sections did not show differences in the morphology of the particles and the matrix before and after exposure (Fig. 5c, d).

The elemental composition measured by EDS for the $50TiO_2$ film after 14 days of exposure at 60 °C is presented in Supplementary Table 7. The distribution of Cr across the depth of the film is reported in Table 3. Cr penetration depth was 30 µm (half of the film thickness) from both sides of the immersed film indicating that the entire film was penetrated.

STEM/EDS analysis was performed in order to determine the exact location of Cr in the film. The lamella prepared for the analysis is presented in Fig. 6. TiO_2 and alumina particles are

clearly visible in the polymer matrix. Examples of manually selected points for EDS analysis at three different areas in the sample (TiO_2, alumina, and polymer matrix) are shown in Fig. 6. Analysis of the matrix showed mainly C and O, with a small amount of Ti and Si found at some points as adventitious contamination. A detailed composition of the film at selected points is presented in Supplementary Table 8. Notably, Cr was identified close to both alumina and titania particles. The origin of Cr in the film was clearly the exposure solution since Cr was not detected within the film before exposure (Supplementary Table 9).

Table 3. Concentration of Cr at different sample depths for $50TiO_2$ film exposed in aqueous Na_2CrO_4 solution for 14 days at 60 °C.

Sample depth (μm)[a]	Cr (wt. %) point 1	Cr (wt. %) point 2	Cr (wt. %) point 3	Cr (wt. %) average	s (±)
3	0.3	0.3	0.1	0.2	0.12
7	0.4	0.5	0.1	0.3	0.21
15	0.5	0.5	0.3	0.4	0.12
30	0.6	0.7	0.5	0.6	0.10

[a]Composition of the film at different depths is reported up to half of its thickness (30 μm); the film was exposed from both sides, hence the maximum migration distance equals to 1/2 of the film thickness.
The thickness of the film was 60 μm.

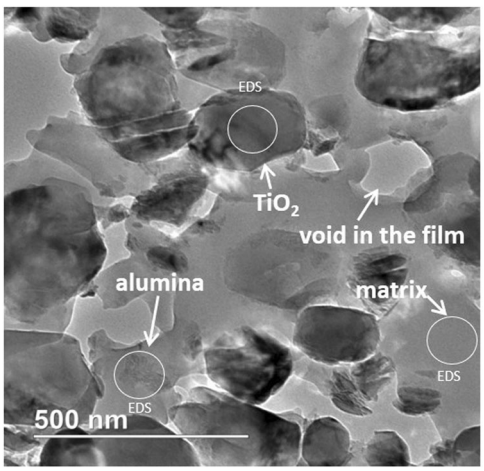

Fig. 6 STEM image of a lamella of 50 TiO_2 film after exposure to the aqueous solution of Na_2CrO_4 for 14 days at 60 °C. The image shows alumina and TiO_2 particles in the polymer matrix (white circles show examples of the areas of acquired EDS spectra).

STEM/EDS spectral images were acquired to analyze the distribution of elements in the film and more importantly to determine where Cr was located. In Fig. 7, the distribution of Cr, Ti (representing TiO_2), and C (representing polymer matrix) is shown. It is evident that Cr is located at the surface of the TiO_2 particles but not in the polymer matrix. This is in contrast to the $30TiO_2$ film exposed to the acetone-contained chromate solution where Cr was found in the matrix. This indicates that chromate transport was promoted by the presence of the connected particles and voids within polymer film pigmented closely to the critical PVC. Similarly, the preferential movement of water through the matrix/particle interface was demonstrated for model systems with microsize glass spheres mimicking pigment particles in polymer coatings[36]. Possible explanations for such phenomenon include the segregation of water and solvated ions on the pigment surfaces[36] or preferential transport via connected pigment pathways where the PVC is above the percolation threshold[35].

In summary, after exposure to purely aqueous solutions, Cr could not be detected under any experimental conditions in $30TiO_2$ films. However, in $50TiO_2$ (PVC of 50%, i.e., close to the critical PVC) Cr was detected at the particle–matrix interface (or on the pigment particles) thus suggesting that in the absence of significant swelling of the polymer matrix, ion transport occurs along the pigment/matrix interface. TiO_2 pigment particles can contribute to forming an interconnected network of particles in anticorrosive coatings, and likely, the mechanism of chromate ion leaching from the anticorrosive pigment particles in the coating can be influenced by such particles included in the formulation. Moreover, different types of additives present in the polymer matrix play a different role in the migration mechanism. In the case of inert TiO_2 pigment, acceleration of chromate ions migration was via the particle/matrix interface of the network of interconnected particles. In contrast, for other type of particles (commonly used filler: $BaSO_4$) studied recently, it was shown that $BaSO_4$ particles were actively contributing to the migration mechanism via the ion-exchange process while slowly leaching from the film[25]. $BaSO_4$ particles were shown to partially dissolve and leach from the films when exposed to chromate solution, leaving the space for the connected transport pathways to be formed. This shows a strong dependence between the role of the particles in the transport mechanism and their chemical nature, hence their interaction with the environment (inert TiO_2 and partially soluble $BaSO_4$). Likely, both types of particles interlocked in a polymer protective coating alongside anticorrosive pigments can contribute to a complex leaching mechanism.

METHODS

Materials and samples preparation

Similarly, as in our previous work[25], free-standing films were prepared from epoxy resin Epikote 828 and hardener Ancamine 2500 (resin:hardener

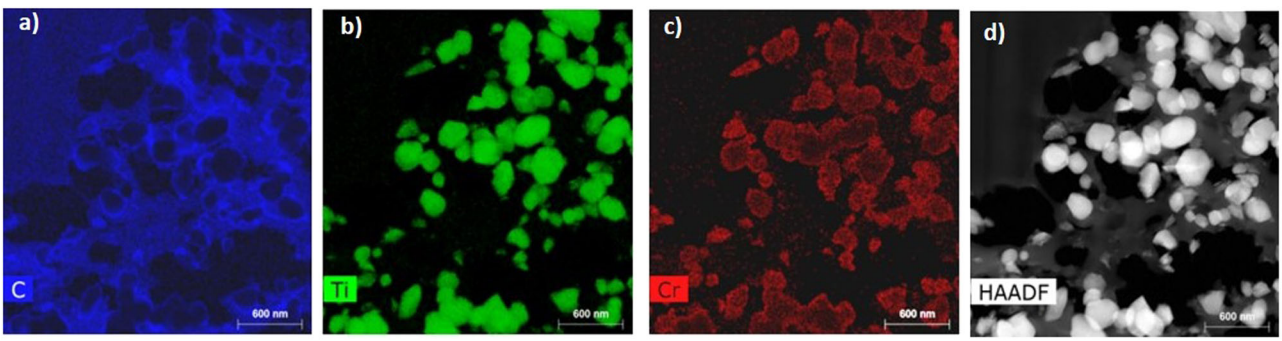

Fig. 7 STEM/EDS analysis of $50TiO_2$ film after 14 days of exposure to aqueous Na_2CrO_4 solution at 60 °C. a–c Distribution of C, Ti, Cr in the selected region of $50TiO_2$ film after exposure to the aqueous solution of Na_2CrO_4 for 14 days at 60 °C. **d** STEM lamella.

weight ratio 1.4:1) with the addition of methyl isobutyl ketone (MIBK) (30 wt. % of the resin and hardener weight). The ingredients were mixed and then applied on polypropylene (PP) plates with a spiral applicator. Films were left to dry overnight at room temperature and then cured at 70 °C for 2 h, which was above the glass transition temperature (T_g) of the polymer (56 °C). The thickness of the dry films was between 60 and 120 µm (100–120 µm for unpigmented films, 100 µm for 30TiO_2 films, and 60 µm for 50TiO_2 films). The samples were cut and peeled off from the PP surface. Unpigmented epoxy and films containing TiO_2 pigment were prepared with PVC of 30 and 50%. Pigmented resins were shaken on a Skandex® paint shaker with solvent and Zirconox® pearls (1.7–2.4 mm) to aid dispersion (the pearls were removed by filtration after mixing), then the hardener was added, and the samples were applied on the substrate and cured as described above. The pigment used was commercially available titanium dioxide TIOXIDE TR92 which contains Al and Zr additives, as reported elsewhere[37].

Exposure and analysis of epoxy films

Free-standing films both unpigmented and pigmented with TiO_2 were exposed for 24 h at 60 °C (slightly above T_g of the tested polymer) to Na_2CrO_4 solutions in water and water/acetone mixture (volume ratio 3:1) at concentrations of 2 mol dm^{-3} and 0.5 mol dm^{-3}, respectively. For pigmented films, extended exposure to the aqueous solution of Na_2CrO_4 for 6 weeks at RT (21 °C) and 14 days at 60 °C was also conducted. The solutions were prepared from Fischer Scientific sodium chromate 99.9%. After exposure, the samples were rinsed with deionized (DI) water and dried above aluminosilicate drying pearls for 24 h.

The film geometry allowed for transport via both sides of the film. It has been assumed that the transport mechanism from both exposed sides is the same and corresponds to the possible transport in the coating applied on a substrate.

SEM/EDS

SEM/EDS was used to study the morphology and composition of the samples before and after exposure. For SEM analysis, unpigmented epoxy films were cross-sectioned using an ultramicrotome (Leica EM UC6) and covered with a 12-nm layer of carbon by sputtering (Leica EM ACE 600). Films with TiO_2 particles were cross-sectioned using broad beam Ar+ ion milling (primary energy 6 keV) (Hitachi High-Technologies Corporation IM4000). Zeiss Crossbeam 540 or Zeiss Sigma 300 coupled to an Oxford Instruments EDS detector were used for SEM imaging at 1, 2, and 5 kV and EDS analysis at 12 kV and 400 pA (aperture 30 µm). The chemical composition based on EDS spectra was calculated with the AZtec software supplied by Oxford Instruments.

The composition of the films after exposure to chromate solution was measured by SEM/EDS at three points within the prepared cross sections (Supplementary Fig. 2). Films were probed at 1/2, 1/4, 1/8, 1/16, and 1/32 of the total film thickness. Not exposed reference films were measured only at 1/2 of the total film thickness.

STEM/EDS

Samples analyzed with STEM/EDS were cut with a Leica EM UC6 ultramicrotome using a diamond knife into thin lamellae with a thickness of ~70 nm and placed on Cu TEM grids. The samples were analyzed using a JEOL2010F-FEG-TEM instrument equipped with a STEM unit and EDS detector from ThermoNoran. EDS data acquisition and evaluation were performed with the Noran System Six software. In EDS spectral images, the lateral resolution was determined by the choice of the number of pixels rather than by the size of the electron beam (1 nm). Typically, the resolution of the spectral images was around 10 nm. In addition, high-angle annular dark-field (HAADF) and dark-field (DF) scanning transmission electron microscope imaging was performed on a Thermo Scientific Talos F200X STEM with a high brightness X-FEG electron source and Super-X energy-dispersive silicon drift detectors (SDDs). The microscopes were operated at an accelerating voltage of 200 kV with beam currents of 0.65 nA and 1 nA, respectively. EDS spectral images were acquired in the Velox software with a typical image size of 1024 × 1024 pixels.

DATA AVAILABILITY

The data that support the findings of this study are available from the corresponding author upon reasonable request.

Received: 8 November 2020; Accepted: 25 January 2021;
Published online: 05 March 2021

REFERENCES

1. Lyon, S. B., Bingham, R. & Mills, D. J. Advances in corrosion protection by organic coatings: what we know and what we would like to know. *Prog. Org. Coat.* **102**, 2–7 (2017).
2. Jadhav, N., Byrom, J., Suryawanshi, A. & Gelling, V. Transport in protective coatings. in Hughes A., Mol J., Zheludkevich M, Buchheit R. (eds), *Active Protective Coatings. Springer Series in Materials Science*. Vol. 233, 299–312 (Springer, 2016).
3. Bierwagen, G. P. & Tallman, D. E. Choice and measurement of crucial aircraft coatings system properties. *Prog. Org. Coat.* **41**, 201–216 (2001).
4. Montemor, M. F. Functional and smart coatings for corrosion protection: a review of recent advances. *Surf. Coat. Technol.* **258**, 17–37 (2014).
5. Kendig, M., Jeanjaquet, S., Addison, R. & Waldrop, J. Role of hexavalent chromium in the inhibition of corrosion of aluminum alloys. *Surf. Coat. Technol.* **140**, 58–66 (2001).
6. Howard, R. L., Zin, I. M., Scantlebury, J. D. & Lyon, S. B. Inhibition of cut edge corrosion of coil-coated architectural cladding. *Prog. Org. Coat.* **37**, 83–90 (1999).
7. Sinko, J. Challenges of chromate inhibitor pigments replacement in organic coatings. *Prog. Org. Coat.* **42**, 267–282 (2001).
8. Visser, P., Terryn, H. & Mol, J. M. C. Aerospace coatings. in Hughes A., Mol J., Zheludkevich M, Buchheit R. (eds), *Active Protective Coatings. Springer Series in Materials Science*, Vol. 233, 315–372 (Springer, 2016).
9. Gharbi, O., Thomas, S., Smith, C. & Birbilis, N. Chromate replacement: what does the future hold? *npj Mater. Degrad.* **2**, 12 (2018).
10. Liu, W., Hoa, S. V. & Pugh, M. Water uptake of epoxy-clay nanocomposites: experiments and model validation. *Compos. Sci. Technol.* **68**, 2066–2072 (2008).
11. Philippe, L., Sammon, C., Lyon, S. B. & Yarwood, J. An FTIR/ATR in situ study of sorption and transport in corrosion protective organic coatings-1. Water sorption and the role of inhibitor anions. *Prog. Org. Coat.* **49**, 302–314 (2004).
12. Jamali, S. S., Suesse, T., Jamali, S., Mills, D. J. & Zhao, Y. Mechanism of ionic conduction in multi-layer polymeric films studied via electrochemical measurement and theoretical modelling. *Prog. Org. Coat.* **108**, 68–74 (2017).
13. Nguyen, T., Hubbar, J. B. & Pommersheim, J. M. Unified model for the degradation of organic coatings on steel in a neutral electrolyte. *J. Coat. Technol.* **68**, 45–56 (1996).
14. Morsch, S., Lyon, S., Smith, S. D., Greensmith, P. & Gibbon, S. R. Mapping water uptake in organic coatings using AFM-IR. *Faraday Discuss.* **180**, 527–542 (2015).
15. Morsch, S., Lyon, S. & Gibbon, S. R. The degradation mechanism of an epoxy-phenolic can coating. *Prog. Org. Coat.* **102**, 37–43 (2017).
16. Prosek, T. & Thierry, D. A model for the release of chromate from organic coatings. *Prog. Org. Coat.* **49**, 209–217 (2004).
17. Scholes, F. H. et al. Chromate leaching from inhibited primers Part I. Characterisation of leaching. *Prog. Org. Coat.* **56**, 23–32 (2006).
18. Hughes, A. E. et al. The application of multiscale quasi 4D CT to the study of SrCrO4 distributions and the development of porous networks in epoxy-based primer coatings. *Prog. Org. Coat.* **77**, 1946–1956 (2014).
19. Hughes, A. E. et al. Using X-ray tomography, PALS and Raman spectroscopy for characterization of inhibitors in epoxy coatings. *Prog. Org. Coat.* **74**, 726–733 (2012).
20. Sellaiyan, S. et al. Leaching properties of chromate-containing epoxy films using radiotracers, PALS and SEM. *Prog. Org. Coat.* **77**, 257–267 (2014).
21. Hughes, A. E. et al. Structure and transport in coatings from multiscale computed tomography of coatings—new perspectives for electrochemical impedance spectroscopy modeling? *Electrochim. Acta* **202**, 243–252 (2016).
22. Hughes, A. E. et al. Revelation of intertwining organic and inorganic fractal structures in polymer coatings. *Adv. Mater.* **26**, 4504–4508 (2014).
23. Hughes, A. E. et al. Diversity of internal structures in inhibited epoxy primers. *AIMS Mater. Sci.* **2**, 379–391 (2015).
24. Kopec, M., Lyon, S. B., Rossenaar, B. D., Gibbon, S. R. & Davies, A. N. Throwing light on corrosion inhibition. *Spectrosc. Eur.* **30/1**, 20–23 (2018).
25. Kopec, M. et al. Chromate ion transport in epoxy films: Influence of $BaSO_4$ particles. *Prog. Org. Coat.* **147**, 105739 (2020).
26. Zallen, R. *The Physics of Amorphous Solids* (Wiley, 1983).
27. Perera, D. Y. Effect of pigmentation on organic coating characteristics. *Prog. Org. Coat.* **50**, 247–262 (2004).
28. Asbeck, W. K. & Van Loo, M. Critical pigment volume relationship. *Ind. Eng. Chem.* **41**, 1470–1475 (1949).
29. Kaplan, M. L. Solvent penetration in cured epoxy networks. *Polym. Eng. Sci.* **31**, 689–698 (1991).
30. Roobottom, H. K., Jenkins, H. D. B., Passmore, J. & Glasser, L. Thermochemical radii of complex ions. *J. Chem. Educ.* **76**, 1570–1573 (1999).

31. Hinteregger, E. et al. Structure and dynamics of the chromate ion in aqueous solution. An ab initio QMCF-MD simulation. *Inorg. Chem.* **49**, 7964–7968 (2010).
32. Geise, G. M., Paul, D. R. & Freeman, B. D. Fundamental water and salt transport properties of polymeric materials. *Prog. Org. Coat.* **39**, 1–42 (2014).
33. van Driel, B. A. et al. New insights into the complex photoluminescence behaviour of titanium white pigments. *Dyes Pigm.* **155**, 14–22 (2018).
34. Goldstein, J. I. et al. *Scanning Electron Microscopy and X-ray Microanalysis*, 3rd edn. (Springer Science+Business Media, 2003).
35. Lekatou, A., Faidi, S. E., Ghidaoui, D., Lyon, S. B. & Newman, R. C. Effect of water and its activity on transport properties of glass/epoxy particulate composites. *Compos. Part A Appl. Sci. Manuf.* **28A**, 223–236 (1997).
36. Donkers, P. A. J., Huinink, H. P., Erich, S. J. F., Reuvers, N. J. W. & Adan, O. C. G. Water permeability of pigmented waterborne coatings. *Prog. Org. Coat.* **76**, 60–69 (2013).
37. Hughes, A. et al. Particle characterisation and depletion of Li_2CO_3 inhibitor in a polyurethane. *Coatings* **7**, 106 (2017).

ACKNOWLEDGEMENTS

Members of the ECG-MAS and ECG-MMT from Nouryon are kindly acknowledged for their contribution to the analytical work related to this project. We would like to thank Lennaert Klerk for the contribution to the project. This work was supported by the European Union's Horizon 2020 research and innovation program under the Marie Sklodowska-Curie grant agreement No 706908.

AUTHOR CONTRIBUTIONS

M.K., B.D.R., A.N.D., and S.B.L.: research goals and methodology. M.K.: film samples preparation, exposure experiments, SEM/EDS measurements and data analysis, writing of the initial draft, paper revision, and writing of the final version. B.D.R.: project supervision, SEM/EDS data analysis. K.L. and A.J.: STEM/EDS data acquisition and analysis. A.N.D. and S.B.L.: scientific supervision of the project. P.V.: film samples preparation. All authors contributed to the progress discussions, and paper revision.

COMPETING INTERESTS

The authors declare no competing interests.

ADDITIONAL INFORMATION

Supplementary information The online version contains supplementary material available at https://doi.org/10.1038/s41529-021-00156-7.

Correspondence and requests for materials should be addressed to M.K.

Reprints and permission information is available at http://www.nature.com/reprints

Publisher's note Springer Nature remains neutral with regard to jurisdictional claims in published maps and institutional affiliations.